



# Characterization of Er<sup>3+</sup>-doped fluoride glass ceramics waveguides containing LaF<sub>3</sub> nanocrystals

Brigitte Boulard<sup>a,\*</sup>, O. Péron<sup>a</sup>, Y. Jestin<sup>b</sup>, M. Ferrari<sup>b</sup>, C. Duverger-Arfulso<sup>a</sup>

<sup>a</sup> Laboratoire des Oxydes et Fluorures, UMR CNRS 6010, Université du Maine, Av. O. Messiaen, 72085 Le Mans, France

<sup>b</sup> CNR-IFN, Istituto di Fotonica e Nanotecnologie, CSMFO Group, via alla Cascata 56/C, 38050 Povo, Italy

## ARTICLE INFO

Available online 5 April 2009

### Keywords:

Fluoride  
Glass ceramics  
Erbium  
Bandwidth  
Luminescence

## ABSTRACT

Highly Er<sup>3+</sup>-doped fluoride glass ceramics planar waveguides containing LaF<sub>3</sub> nanocrystals have been fabricated by physical vapor deposition (PVD). The solubility of Er<sup>3+</sup> in the segregated nanocrystals can reach 30 mol% which is much larger than the value found in LaF<sub>3</sub>-oxide glass ceramics. A quantitative analysis of the photoluminescence of the 1.54 μm emission band of Er<sup>3+</sup> ions has demonstrated that erbium ions are partitioned in both crystals and vitreous phase. The short lifetime (2.2 ms) measured for erbium incorporated in LaF<sub>3</sub> crystal lattice is a consequence of concentration quenching while the lifetime is close to 10 ms in the glassy phase. The emission bandwidth has been found to be greater than that of the precursor glass (71 nm at the half-height width). The high Er<sup>3+</sup> concentration and spectral width could make this nanostructured fluoride material suitable for planar amplifier in the C telecommunication band.

© 2009 Elsevier B.V. All rights reserved.

## 1. Introduction

Rare-earth-doped transparent glass ceramics (GC) have a great interest in the area of optical devices, taking benefit of macroscopic glass properties and crystal-like spectroscopic characteristics of fluoride material: low phonon energy, high solubility of rare-earth ions, and flat broad emission spectrum of Er<sup>3+</sup> at 1.5 μm. Early works of Auzel [1] and more recently of Mortier [2] have demonstrated the ability of heavy metal fluoride glasses ZELA and ZELAG (54–60ZrF<sub>4</sub> 6–10ErF<sub>3</sub> 25–29LaF<sub>3</sub> 1–6AlF<sub>3</sub> 0–6GaF<sub>3</sub> in mol%) to give highly crystalline (>90%) and transparent glass ceramics, by heat treatment at 70 °C above the glass transition temperature T<sub>g</sub> (~390 °C). In glass ceramics, the crystallites have to be small enough to avoid scattering losses; in general, one considers that the diameter has to be lower than λ/10, that is <100 nm for infra-red application.

In order to develop size-reduced devices as integrated optical amplifiers (IOA) and microlasers, vapor phase processes (PVD, RF sputtering, pulse laser deposition...) have been developed to reproduce the composition and optical properties of bulk material in thin films. The PVD process permits to fabricate fluoride glass planar waveguides, with good guiding properties (propagation loss ~0.5 dB/cm [3]) and spectroscopic properties equivalent to bulk.

The ability to fabricate ZELA glass ceramics waveguides containing LaF<sub>3</sub> nanocrystals have been reported recently in Ref. [4]. This paper presents further developments in the spectroscopic characterization of these waveguides. The aim of the study is to estimate the fraction of Er<sup>3+</sup> in crystalline and vitreous phases as function of deposition temperature. The influence of the homogeneously distributed nanocrystals on lifetime and emission broadness of the <sup>4</sup>I<sub>13/2</sub>→<sup>4</sup>I<sub>15/2</sub> transition of the Er<sup>3+</sup> ion is also investigated.

## 2. Experimental

Owing to the large vapor pressure gap between the ZrF<sub>4</sub> and rare-earth fluorides (at least height orders of magnitude), the evaporation was conducted using two separate crucibles, one containing a fluoride glass (ZBNA) as source of ZrF<sub>4</sub> and AlF<sub>3</sub>, the other one containing a mixture of LaF<sub>3</sub> and ErF<sub>3</sub>, heated respectively at 520 and 1335 °C. The evaporation of La<sub>(1-x)</sub>Er<sub>x</sub>F<sub>3</sub> being non-congruent [4], the starting composition was fixed at x = 0.45, leading to a binary deposit with x = 0.3. The substrate, a CaF<sub>2</sub> single-crystal oriented plate was heated and put in rotation over the two crucibles, to provide homogeneous thickness and composition for the ZELA thin films. Different ZELA films were synthesized with increasing substrate temperature, from 390 to 460 °C. The duration of the evaporation was 40 min leading to films ~2 μm thick. A film containing only ErF<sub>3</sub> and LaF<sub>3</sub> was also produced for spectroscopic investigations.

\* Corresponding author. Tel.: +33 2 43 83 33 70.

E-mail address: [brigitte.boulard@univ-lemans.fr](mailto:brigitte.boulard@univ-lemans.fr) (B. Boulard).

X-ray analysis (XRD) was carried out with a powder diffractometer, using a Cu anode in the  $10\text{--}60^\circ$   $2\theta$  mode, to control the devitrification and identify the crystalline phases.

The propagation losses of the waveguides were estimated in the visible (at 633 nm) and in the infra-red (at 1340 nm) out of the erbium absorption bands, from the diffusion profile curve obtained using a m-line apparatus based on prism coupling (Metricon 2010).

The photoluminescence measurements of the  $^4I_{13/2} \rightarrow ^4I_{15/2}$  transition of the  $\text{Er}^{3+}$  ions were performed using the 514.5 nm line of an Argon-ion laser as excitation source, and dispersing the luminescence light with a 320 mm single-grating mono-chromator with a resolution of 2 nm. The waveguiding mode of the samples was excited by prism coupling and the light was detected using an InGaAs photodiode and a lock-in technique. Decay curves were obtained by chopping the CW exciting beam and recording the signal with an oscilloscope. All the measurements were performed at room temperature.

### 3. Results and discussion

The XRD of ZELA waveguides are presented in Fig. 1 as function of the deposition temperature. Crystallization of an hexagonal  $\text{LaF}_3$ -related phase is observed for temperature higher than  $430^\circ\text{C}$ . More precisely, the diffraction peaks match the solid solution  $\text{La}_{0.7}\text{Er}_{0.3}\text{F}_3$  pattern (PDF file 04-006-9851) that is the composition of the vapor resulting from the non-congruent evaporation of rare-earth mixture. Therefore, the  $\text{Er}^{3+}$  concentration in  $\text{LaF}_3$  crystal obtained by PVD goes largely beyond the intrinsic solubility limit (1 mol% [5]) and is close to the solubility achieved by quenching of single crystal from the melt in water [5] but much higher than the value found in  $\text{LaF}_3$ -oxide glass ceramics (1.5 mol% [6]). Thus it appears that the doping of the crystals can be easily controlled via the composition of the starting mixture of rare-earth fluorides that is evaporated.

Unlike bulk glass which undergoes spinodal decomposition after heat treatment [2] with a crystal-phase composition close to the precursor glass, classical nucleation seems to occur in ZELA films; high-resolution transmission electronic microscopy (TEM) image shows highly connected  $\text{Er}^{3+}$ -doped  $\text{LaF}_3$  nanocrystals less than 50 nm in size (Fig. 1). The most likely explanation for the

different behaviour between bulk (prepared by classical melting–quenching process) and films obtained by PVD is that “aggregates” of  $\text{ErF}_3$  and  $\text{LaF}_3$  formed in the vapor state, remain at a nano- or sub-nanoscale as the vapor is quenched on the substrate; they probably act as nucleation agents.

The waveguides show interesting guiding properties (Table 1) and the presence of nanocrystals in the glass ceramics waveguides induces negligible loss in the infra-red with respect to the glassy waveguide (1.3 dB/cm at 1340 nm). The behaviour is different at 633 nm where the particles diameter is in the range of  $\lambda/10$ : the rise of propagation loss is consistent with an increase of the volume fraction of crystal, except for the waveguide deposited at  $460^\circ\text{C}$ . This can be related to significant particle–particle interaction [7]. No guiding property is observed for the  $\text{La}_{0.7}\text{Er}_{0.3}\text{F}_3$  film at any of the two wavelengths.

In order to study the influence of nanocrystals on the spectroscopic properties of  $\text{Er}^{3+}$  ions, we first compared the luminescence spectra of the precursor glass and of  $\text{La}_{0.7}\text{Er}_{0.3}\text{F}_3$  crystal. The spectra on Fig. 2 reveal a broader emission from  $\text{Er}^{3+}$ -doped  $\text{LaF}_3$  crystal as compared with glass and the luminescence band is red-shifted. While the inhomogeneous broadening in glass is a consequence of the existence of several  $\text{Er}^{3+}$  sites, some internal lattice strain due to the size mismatching of  $\text{La}^{3+}$  and  $\text{Er}^{3+}$  ions, respectively, 132 and 114 pm in eightfold coordination [8], may be evoked to explain the very large bandwidth, through the increase of both the excited- and ground-state splitting (up to a few hundred  $\text{cm}^{-1}$  [9]). Glass ceramics waveguides exhibit an even broader luminescence band than  $\text{LaF}_3$  crystal (Table 2) that increases with substrate temperature; the half-height width (FWHM) reaches 71 nm for deposition conducted at  $460^\circ\text{C}$ . Moreover, the emission is flattened in comparison to precursor glass. Similar broad and flat band has already been reported by V.K. Tikhomirov in oxyfluoride glass ceramics containing  $\text{PbF}_2$  crystals [10]. The observed spectra features should thus mark this

**Table 1**

Propagation losses ( $\pm 0.3$  dB/cm) of ZELA waveguides measured at 633 and 1340 nm as function of substrate temperature.

$T_{\text{substrate}} (^\circ\text{C})$	390	400	430	445	460
633 nm	1.7	1.6	2.9	3.4	2
1340 nm	–	1.2	1.8	1.6	1.3

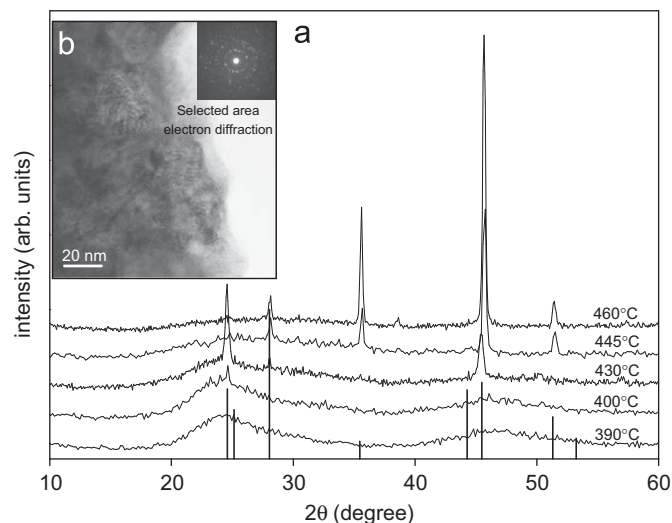


**Fig. 1.** (a) X-ray diffraction patterns of ZELA films obtained by physical vapor deposition as function of deposition temperature. Bars represent the diffraction pattern of  $\text{La}_{0.7}\text{Er}_{0.3}\text{F}_3$  crystalline phase and bar lengths the peak intensities and (b) high-resolution TEM image of glass ceramic waveguide.

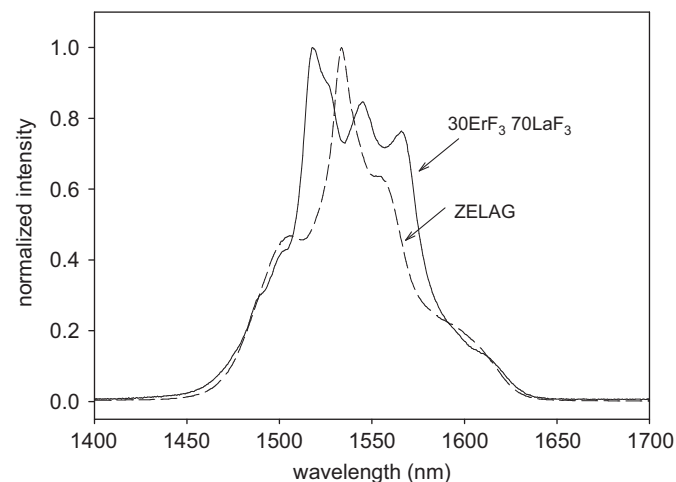


**Fig. 2.** Normalized luminescence spectra from the  $^4I_{13/2} \rightarrow ^4I_{15/2}$  transition of  $\text{La}_{0.7}\text{Er}_{0.3}\text{F}_3$  and bulk ZELAG glass (10 mol%  $\text{Er}^{3+}$ ) obtained after excitation at 514.5 nm.

**Table 2**

Comparison of luminescence characteristics of the  $^4I_{13/2}$  erbium level of  $\text{Er}^{3+}$  in ZELAG bulk glass, ZELA waveguides and  $\text{La}_x\text{Er}_{1-x}\text{F}_3$  film: bandwidth ( $\pm 0.5$  nm), estimation of fraction of erbium in crystal sites from emission spectra shape ( $\propto b/(a+b)$ ) and lifetimes ( $\tau_1$ ,  $\tau_2$ ) of the two decay rate components.

	ZELAG bulk	ZELA waveguides					$\text{La}_x\text{Er}_{1-x}\text{F}_3$ film
$T_{\text{substrate}}$ ( $^{\circ}\text{C}$ )	–	390	400	430	445	460	460
$\text{Er}^{3+}$ (mol%)	10	9	13.4	9.8	10.4	14.5	30
FWHM (nm)	46	53	58	62	62	71	66.5
$b/(a+b)$ (%)	0	9	13	14	25	41	100
Lifetime (ms)							
$\tau_1$	–	$2.5 \pm 0.2$	$2.2 \pm 0.1$	$2.4 \pm 0.1$	$2.7 \pm 0.1$	$2.3 \pm 0.1$	$2.5 \pm 0.5$
$\tau_2$	$10.2 \pm 0.5^a$	$7.6 \pm 0.1$	$10.3 \pm 0.1$	$10.6 \pm 0.1$	$10.5 \pm 0.1$	$9.2 \pm 0.1$	–

<sup>a</sup> Measured on powdered sample.

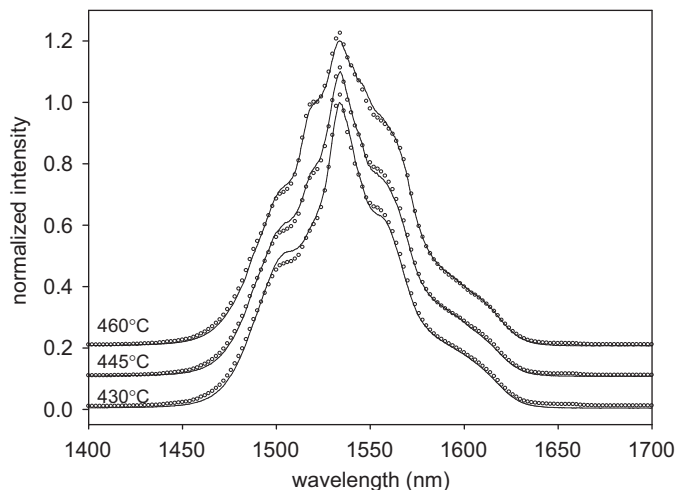


**Fig. 3.** Normalized luminescence spectra from the  $^4I_{13/2} \rightarrow ^4I_{15/2}$  transition of ZELAG waveguides with increasing deposition temperature after excitation at 514.5 nm—experimental, oooo simulation using Eq. (1).

waveguide as a material to receive special consideration for amplification in the 1.54  $\mu\text{m}$  telecommunication window.

The experimental spectra of the glass ceramic can be accurately simulated by the linear combination of crystal and glass spectra using the formula

$$I_{\text{CC}}^{\text{N}}(\lambda) = aI_{\text{glass}}^{\text{N}}(\lambda) + bI_{\text{crystal}}^{\text{N}}(\lambda), \quad (1)$$

where  $I^{\text{N}}(\lambda)$  is the intensity of the normalized spectrum. The result of the simulation is shown in Fig. 3. Since the absorption cross sections are not measurable on thin films, we cannot reach the quantitative fraction of  $\text{Er}^{3+}$  in both crystalline and glassy phase but at least we can see from Table 1 that the fraction of erbium in crystal ( $\propto b/(a+b)$ ), continuously increases with deposition temperature. The broadening of the emission band with deposition temperature is thus related to the increase of the fraction of crystals that exhibits strong splitting and spectral redshift as compared to the precursor glass.

Fig. 4 shows the luminescence decay of the  $^4I_{13/2}$  level of the  $\text{Er}^{3+}$  ion in glass and glass ceramic waveguides and in  $\text{La}_{0.7}\text{Er}_{0.3}\text{F}_3$  film; for the latter, the accuracy is less because of poor light guiding. The decay curves are clearly not single exponential, except for  $\text{La}_{0.7}\text{Er}_{0.3}\text{F}_3$  for which the lifetime is 2.5 ms. In the case of non-single exponential, the decay can be fitted using two exponential components: one with a fast decay rate close to 2.5 ms and the other with a slower decay rate (Table 2)

$$\frac{I(t)}{I(t=0)} = A_1 \exp\left(-\frac{t}{\tau_1}\right) + A_2 \exp\left(-\frac{t}{\tau_2}\right). \quad (2)$$

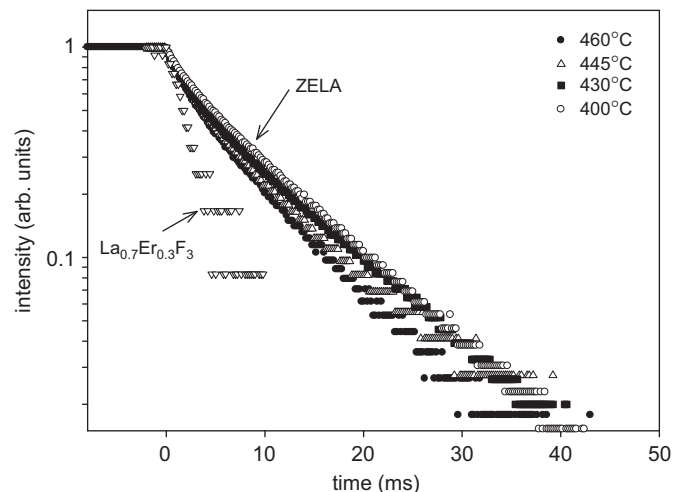


**Fig. 4.** Decay curves (vertical scale log) of the luminescence from the  $^4I_{13/2}$  state of  $\text{Er}^{3+}$  ions in glassy waveguide ( $T_{\text{substrate}} = 400^{\circ}\text{C}$ ), glass ceramic waveguides ( $T_{\text{substrate}}$  from 430 to 460  $^{\circ}\text{C}$ ) and  $\text{La}_{0.7}\text{Er}_{0.3}\text{F}_3$  film upon 514.5 nm excitation.

The fast decay component of ZELA waveguides is unambiguously attributed to  $\text{Er}^{3+}$  in the crystals, the value of lifetime  $\tau_1$  being similar to the one of pure  $\text{La}_{0.7}\text{Er}_{0.3}\text{F}_3$  film. The slower decay rate is thus related to  $\text{Er}^{3+}$  in the glassy phase. For substrate temperature equal to  $T_g$  (i.e., 390  $^{\circ}\text{C}$ ), the lifetime related to the glassy phase is limited by OH quenching groups [4], the film being sensitive to atmospheric moisture: at high temperature, the lifetime reaches the value measured for powdered (to eliminate radiative trapping) glass with similar  $\text{Er}^{3+}$  concentration ( $\sim 10$  ms). The decrease of lifetime from glassy to crystalline phase is probably due to a concentration quenching effect, the  $\text{Er}^{3+}$  concentration being 30 mol% in nanocrystal and  $\sim 10$  mol% in the glassy phase (the radiative lifetime of  $\text{Er}^{3+}$ – $\text{LaF}_3$  single crystal is 12.3 ms [5]). For the glassy phase, no significant concentration quenching is detected despite a high doping level, the lifetime of ZELAG matrix at low concentration (1 mol%) being 11.2 ms [11].

#### 4. Conclusion

Fluoride glass ceramics planar waveguides were fabricated by PVD with a  $\text{LaF}_3$  crystal phase. The good guiding properties in the infra-red, similar to the uncrystallized waveguide, were due to the small,  $< 50$  nm, crystallites. XRD analysis and luminescence spectroscopy demonstrated that the  $\text{Er}^{3+}$  active ion is present in both  $\text{LaF}_3$  nanocrystals and glassy phase. The lifetime of  $\text{Er}^{3+}$  in the crystal phase decreases drastically from  $\sim 10$  ms (in the precursor glass) to 2.5 ms, because of a strong concentration quenching effect. The fraction  $\text{LaF}_3$  nanocrystals increases with deposition

temperature; the doping rate of the nanocrystals remaining constant ( $\sim 30$  mol%) as shown by the values of the lifetime of the fast decay component.

The crystal composition seems to be controlled by the vapor generated by the evaporation of the rare-earth fluoride starting mixture. Therefore, substitution of  $\text{Er}^{3+}$  by  $\text{Yb}^{3+}$  and  $\text{Ce}^{3+}$  ions in the  $\text{LaF}_3\text{-ErF}_3$  mixture will be considered to enhance luminescence properties by (i) reducing concentration quenching, (ii) increasing absorption at 980 nm (wavelength of commercial pump [12]) and (iii) reducing upconversion emission by emptying the  $^4I_{11/2}$  level of  $\text{Er}^{3+}$  through cross relaxation with  $\text{Ce}^{3+}$  [13]. The fabrication of such tri-doped glass ceramic waveguide will be promising for future optical applications around 1.54  $\mu\text{m}$ , owing to the broadness and relative flatness of the emission band observed in this work.

### Acknowledgements

The authors are grateful to the French council Pays de la Loire through the project “MAPS” and to the CNR-CNRS

cooperation program (Contract no. 19141) for their financial support.

### References

- [1] K.E. Lipinska-Kalita, F. Auzel, P. Santa-Cruz, J. Non-Cryst. Solids 204 (1996) 188.
- [2] M. Mortier, A. Montéville, G. Patriarche, J. Non-Cryst. Solids 284 (2001) 85.
- [3] Y. Gao, B. Boulard, M. Couchaud, I. Vasilief, S. Guy, C. Duverger, B. Jacquier, Opt. Mater. 28 (2006) 195.
- [4] O. Péron, B. Boulard, Y. Jestin, M. Ferrari, C. Duverger-Arfulso, S. Kodjikian, Y. Gao, J. Non-Cryst. Solids 354 (2008) 3586.
- [5] G.A. Kumar, R. Riman, E. Snitzer, J. Appl. Phys. 95 (2004) 40.
- [6] F. Goutaland, P. Jander, W.S. Brocklesby, G. Dai, Opt. Mater. 22 (2003) 383.
- [7] M.J. Dejneka, J. Non-Cryst. Solids 239 (1998) 149.
- [8] A.A. Kaminskii, Laser Crystal: Their Physics and Properties, Springer, Berlin, 1990.
- [9] L.M. Krygin, G.N. Neilo, A.D. Prokhorov, Sov. Phys. Solid State 28 (1986) 634.
- [10] V.K. Tikhomirov, D. Furniss, A. Seddon, I.M. Reaney, M. Beggiora, M. Ferrari, M. Montagna, R. Rolli, Appl. Phys. Lett. 81 (2002) 1937.
- [11] O. Péron, PhD thesis, Université du Maine, France (2007).
- [12] O. Péron, C. Duverger-Arfulso, Y. Jestin, B. Boulard and M. Ferrari, Opt. Mater., in press, corrected proof available online 17 November 2008.
- [13] C. Strohhofer, A. Polman, Opt. Mater. 17 (2001) 445.